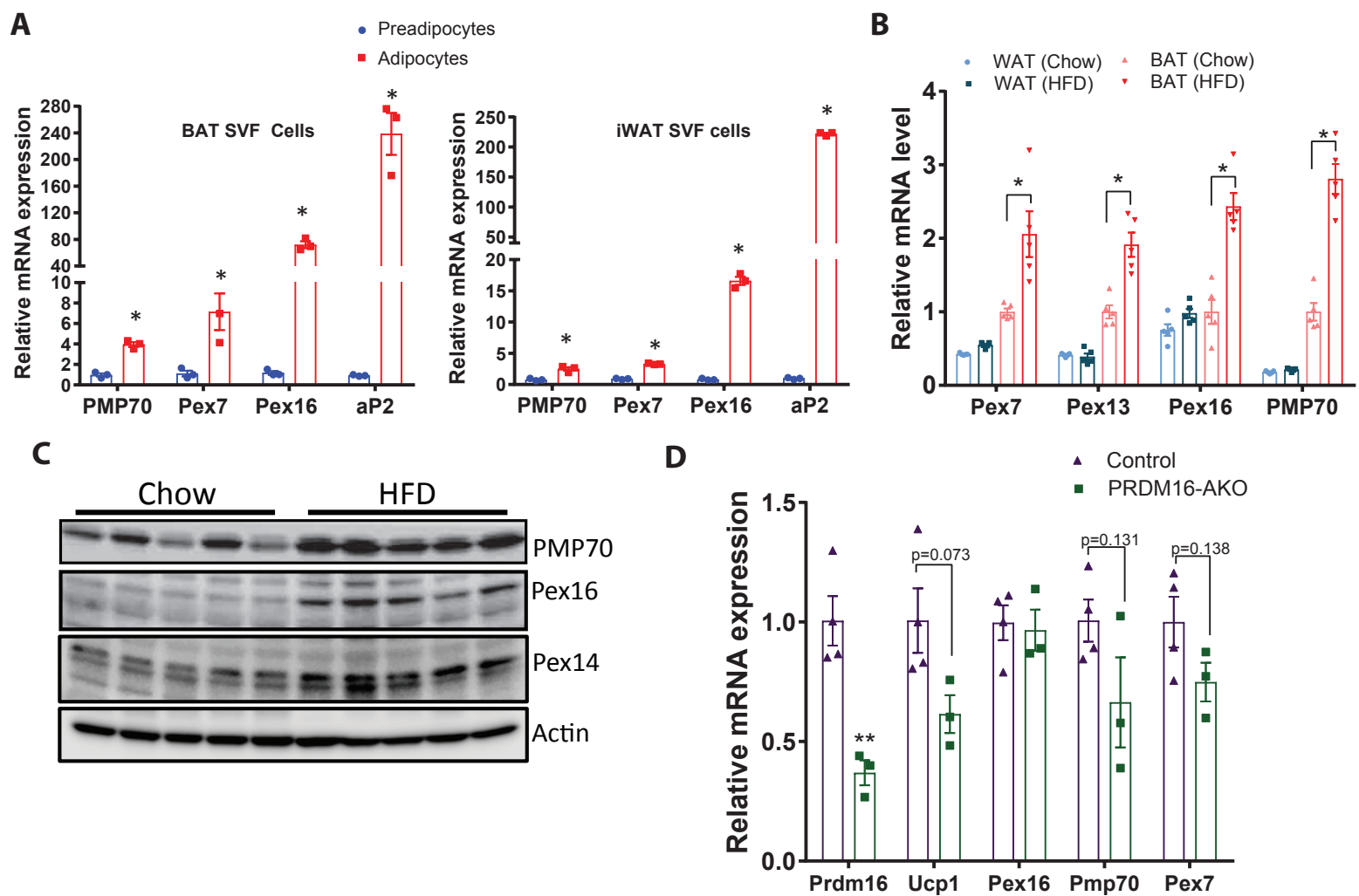


Supplemental Material for:

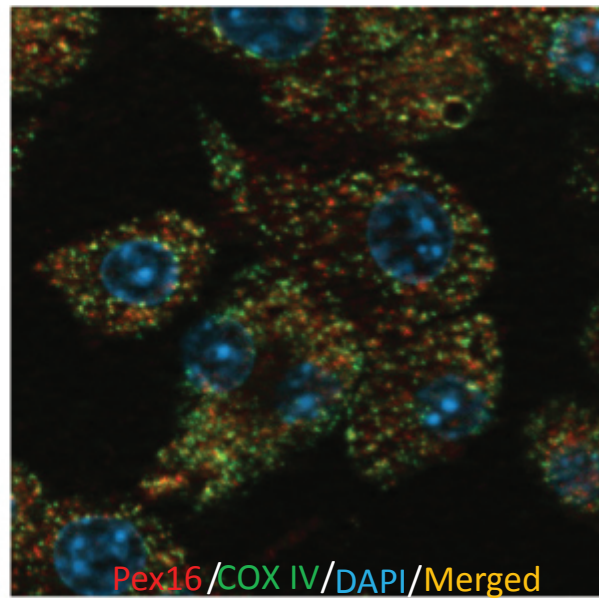
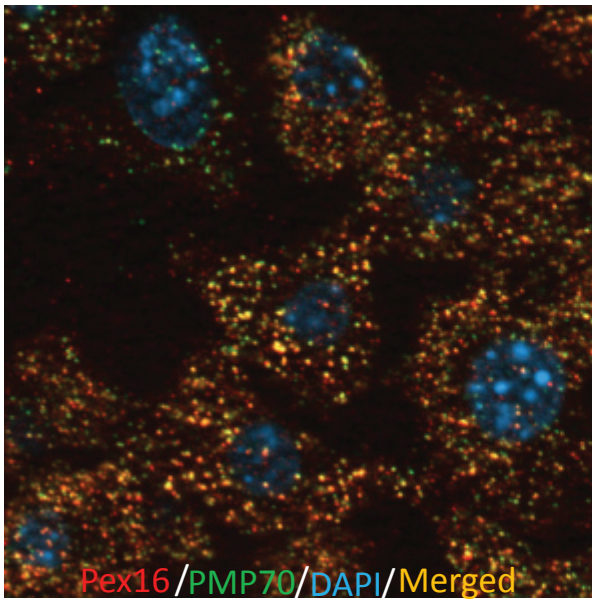
Peroxisome-derived lipids regulate adipose thermogenesis by mediating cold-induced mitochondrial fission

Hongsuk Park, Anyuan He, Min Tan, Jordan M. Johnson, John M. Dean, Terri A. Pietka, Yali Chen, Xiangyu Zhang, Fong-Fu Hsu, Babak Razani, Katsuhiko Funai, and Irfan J. Lodhi

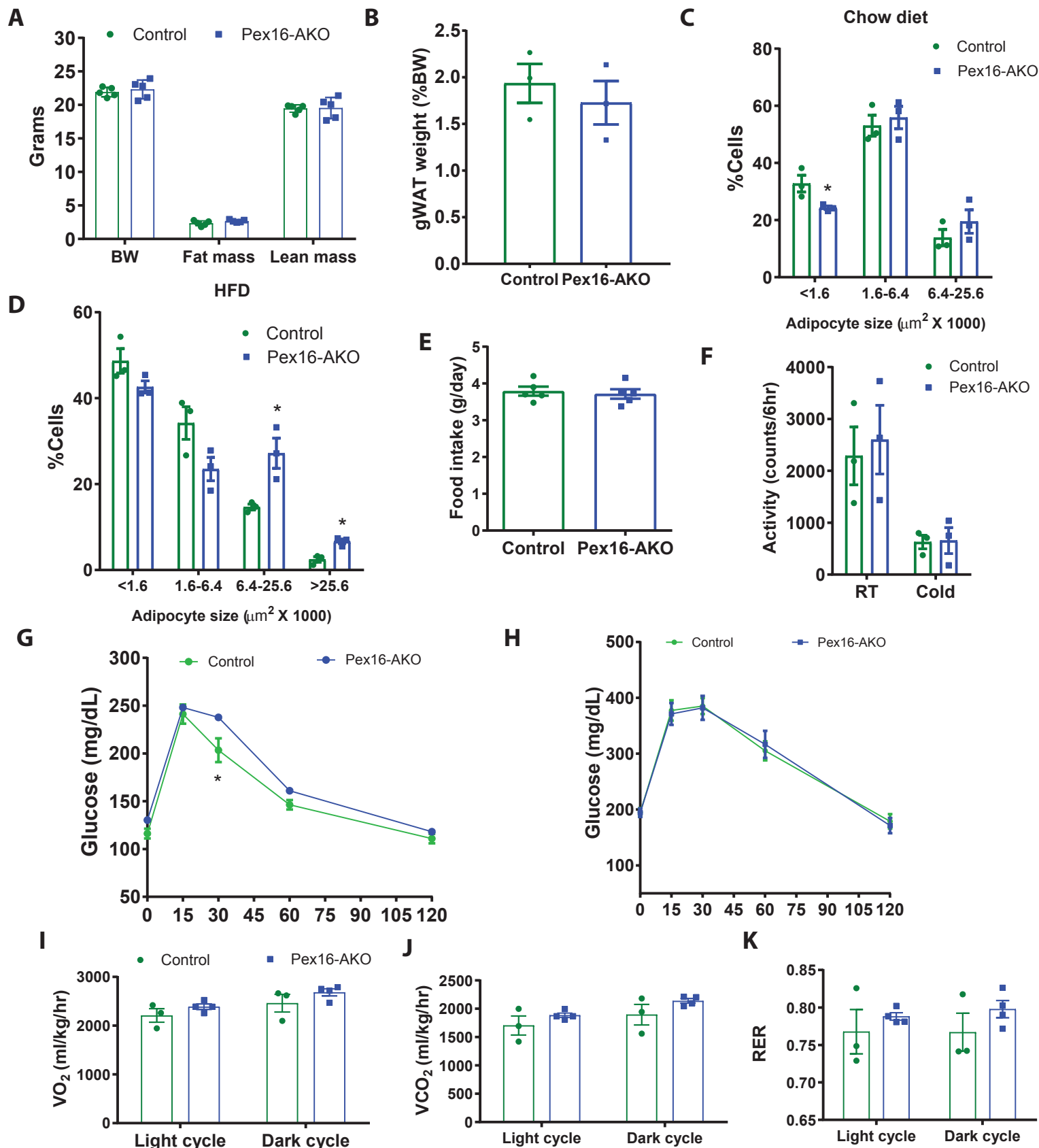


Supplemental Figure 1. Peroxisomal biogenesis factors increase during adipogenesis and with high fat feeding.

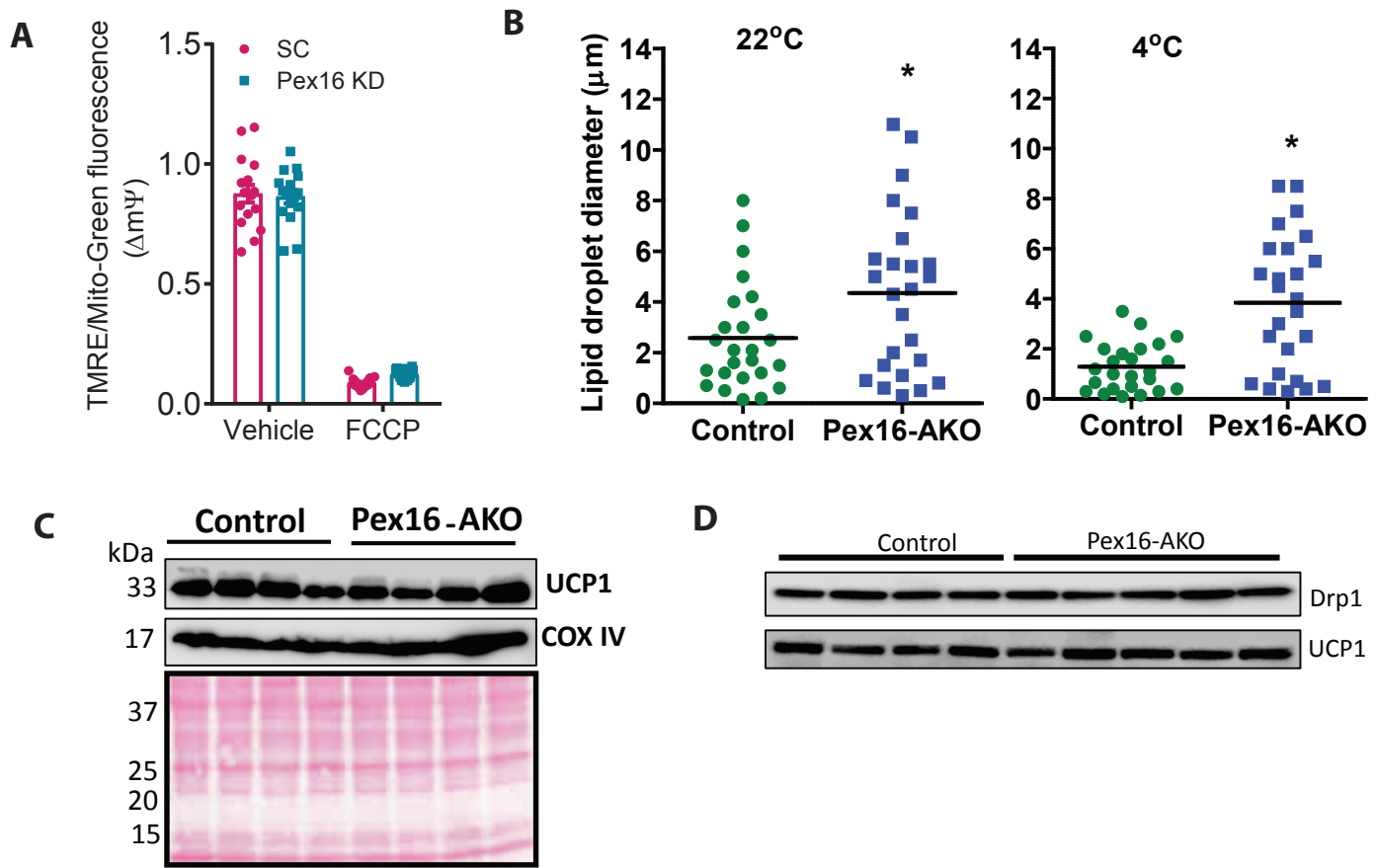
(A) mRNA levels of peroxisomal biogenesis genes and aP2 in BAT and iWAT stromal vascular fraction cells before and after adipogenesis; n=3. (B) mRNA levels of peroxisomal biogenesis genes in gWAT and BAT of wild-type C57 mice fed normal chow diet or high fat diet (HFD) for 8 weeks; n=5. (C) Western blot analysis in BAT of C57 mice fed chow or HFD for 8 weeks. Each lane represents a separate mouse. (D) Gene expression analysis in BAT of PRDM16-AKO and control mice subjected to cold exposure for 2 days; n=3-4. Data are expressed as mean±SEM and were analyzed by Student's t-test; *p<0.05



Supplemental Figure 2. Immunofluorescence analysis of Pex16 in brown adipocytes. Immortalized BAT SVF cells were differentiated into adipocytes and immunostained using a rabbit polyclonal anti-Pex16 antibody together with either mouse monoclonal anti-PMP70 or mouse monoclonal anti-COX IV antibody. Following incubation with fluorescently-tagged secondary antibodies, the cells were analyzed using a Zeiss Axio Imager Z2 fluorescent microscope.

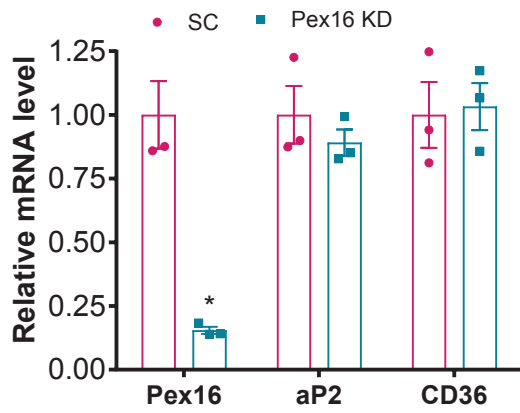


Supplemental Figure 3. Characterization of Pex16-AKO mice. (A) Body composition analysis in chow fed control and Pex16-AKO mice; n=5. (B) Weight of gWAT depots in chow fed mice; n=3. (C-D) Adipocyte size distribution in chow or HFD fed mice based on sizing data obtained using a Beckman Coulter Multisizer III; n=3. (E) Food intake in chow fed mice; n=5. (F) Physical activity measured at normal room temperature and in the cold using an InfraMot TSE system; n=3. (G) GTT in mice fed normal chow diet; n=11. Error bars in Pex16-AKO mice are smaller than the symbols. (H) GTT in mice fed HFD diet for 14 weeks; n=10-11. (I-K) Measurement of VO₂, VCO₂ and respiratory exchange ratio (RER) in Pex16-AKO and control mice fed HFD for 15 weeks; n=3-4. Data are expressed as mean±SEM and were analyzed by Student's t-test; *p<0.05.

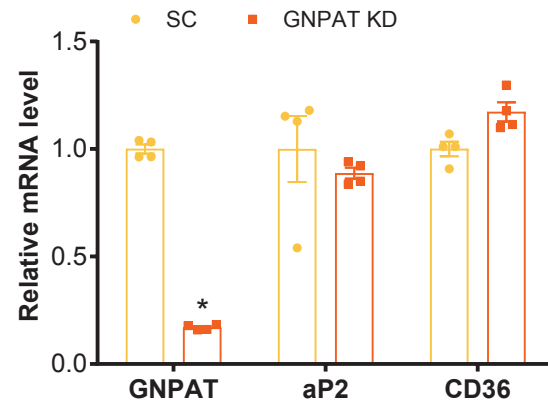


Supplemental Figure 4. Effects of Pex16 inactivation on mitochondria and lipid droplets in brown and beige adipocytes. (A) Mitochondrial membrane potential measured using TMRE in differentiated BAT SVF cells treated with scrambled or Pex16 shRNA, followed by incubation with FCCP or vehicle control. TMRE fluorescence was normalized to MitoTracker Green fluorescence; $n=16$ per condition. (B) Diameter of lipid droplets measured in TEM images of BAT from control and Pex16-AKO mice kept at room temperature or subjected to cold exposure for 2 days. (C) Western blot analysis of UCP1 and COX IV protein expression in control and Pex16-AKO mice subjected to cold exposure for 2 days. Each lane represents a separate mouse. (D) Western blot analysis of Drp1 and UCP1 levels in the mitochondrial fractions isolated from BAT of control and Pex16-AKO mice subjected to cold exposure for 2 days. Each lane represents a separate mouse. Data in panels A and B are expressed as mean \pm SEM and were analyzed by Student's t-test. * $P<0.05$.

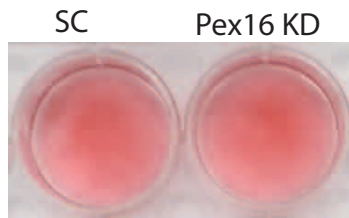
A.



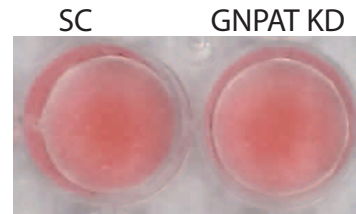
C.



B.

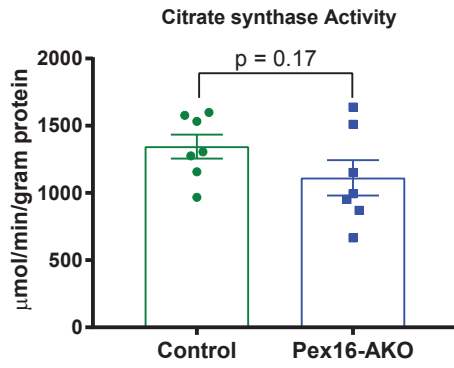


D.

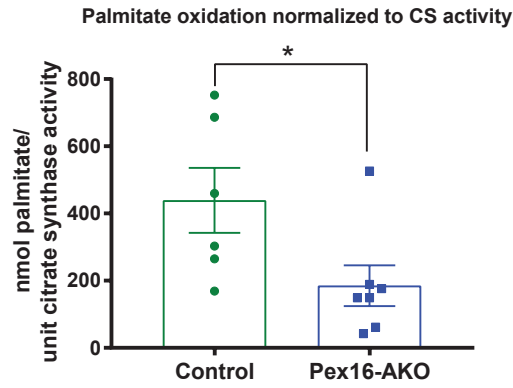


Supplemental Figure 5. Effect of Pex16 or GNPAT knockdown on adipogenesis. (A and C) Immortalized BAT SVF cells were subjected to adipogenesis for 4 days and then treated with the indicated shRNA and analyzed for gene expression 5 days later. (B and D) Oil red O staining in the cells in panels A and C. Data in panels A and C are expressed as mean±SEM and were analyzed by Student's t-test. *P<0.05.

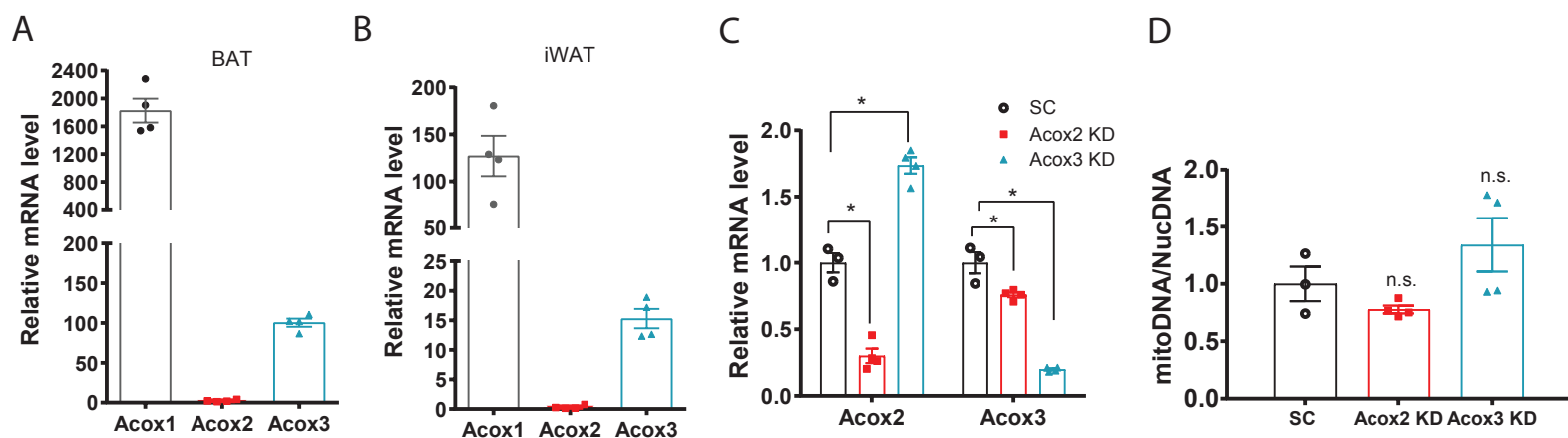
A



B

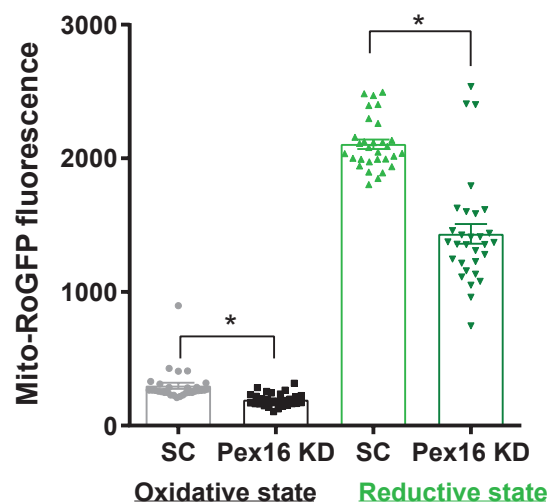


Supplemental Figure 6. Measurement of citrate synthase activity and palmitate oxidation. (A) Citrate synthase activity measured in homogenates of BAT from Pex16-AKO and control mice; n=7. (B) Palmitate oxidation normalized to citrate synthase activity in BAT; n=6-7. Data are expressed as mean±SEM and were analyzed by Student's t-test; *p<0.05.

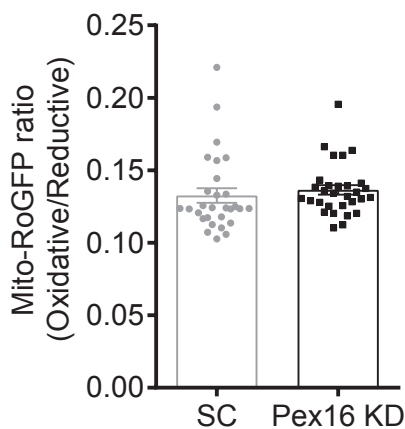


Supplemental Figure 7. Relative expression levels of Acox2 and Acox3 and effects of their knockdown on mtDNA content. (A-B) Relative mRNA levels of Acox1, Acox2, and Acox3 in BAT and iWAT of wild-type C57 mice; n=3. (C) mRNA levels of Acox2 or Acox3 in BAT SVF cells following treatment with SC, Acox2, or Acox3 shRNA.; n=3-4. (D) mtDNA content normalized to nuclear DNA in the cells in panel C; n=3-4. Data are expressed as mean±SEM and were analyzed by Student's t-test. *P<0.05; n.s., not significant.

A

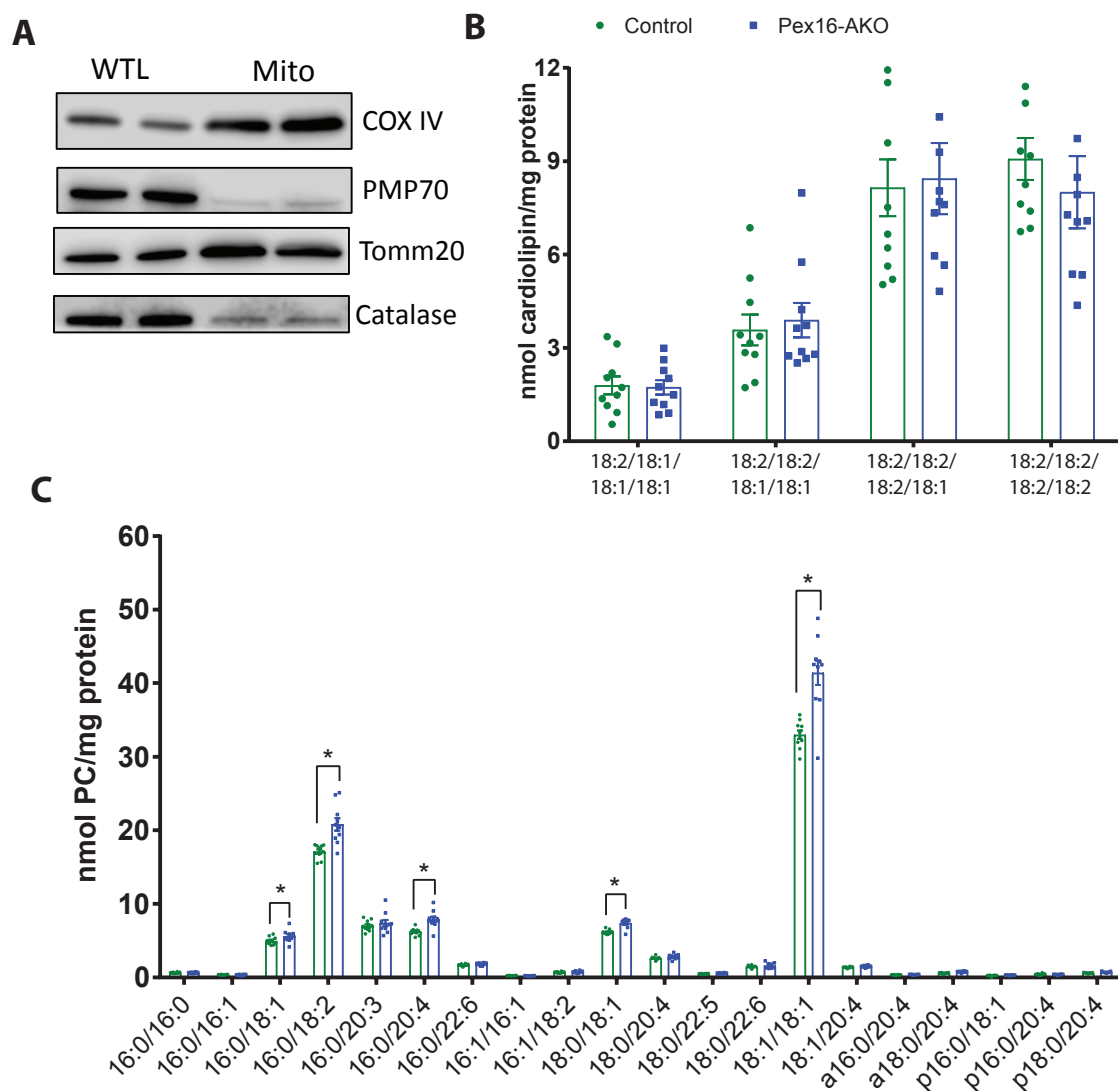


B

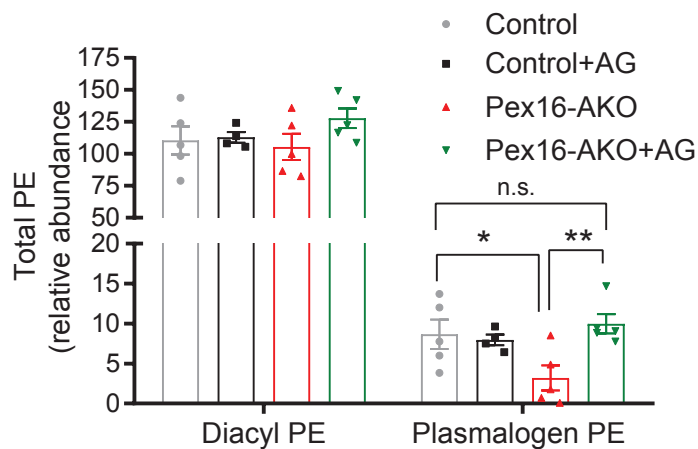
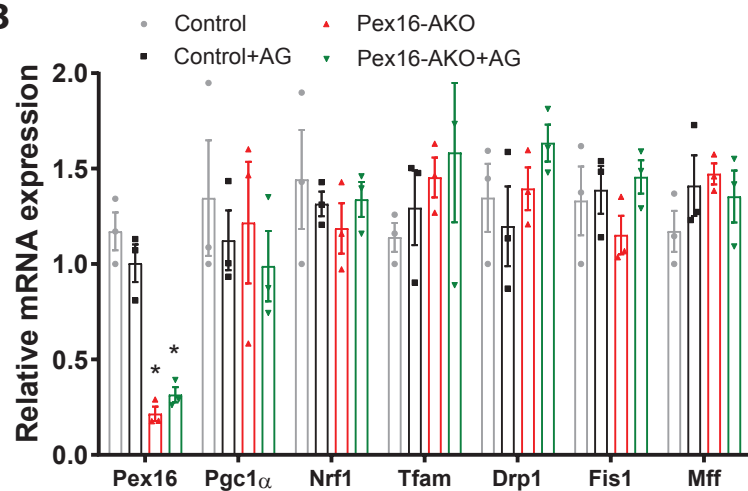
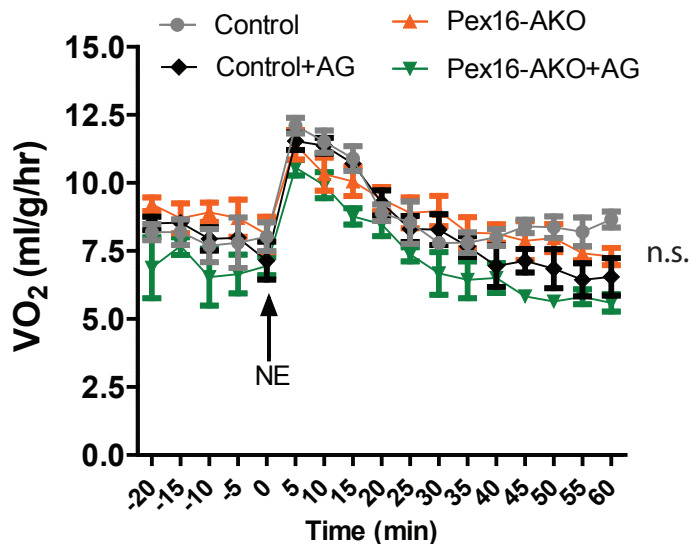
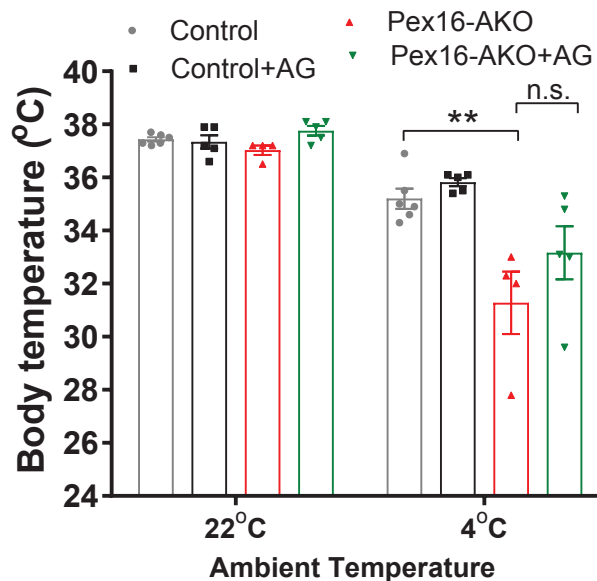


Supplemental Figure 8. Measurement of mitochondrial ROS production using a ratiometric redox sensor.

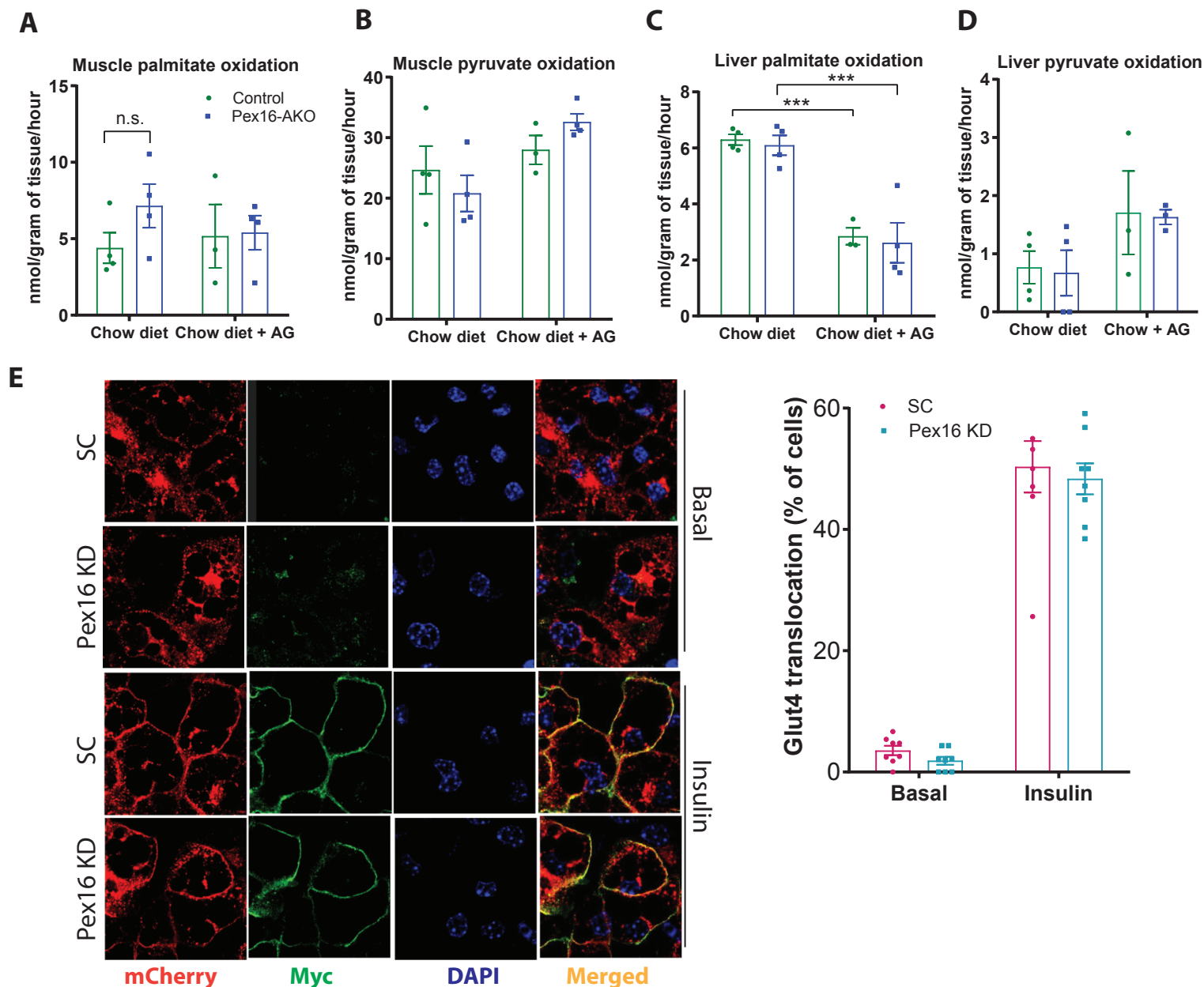
(A) Immortalized BAT SVF cells stably expressing lentiviral-encoded mito-RoGFP were differentiated into adipocytes and treated with SC or Pex16 shRNA. GFP fluorescence was measured following excitation at 400 nm (oxidative state) or at 490 nm (reductive state). (B) Ratio of the fluorescence measured in panel A. Data are expressed as mean ± SEM and were analyzed by Student's t-test; * $p < 0.05$; n.s., not significant.



Supplemental Figure 9. Mass spectrometric analysis of mitochondrial phospholipids. (A) Western blot analysis of whole tissue lysate (WTL) and mitochondrial fraction from BAT of control and Pex16 AKO mice. (B-C) Levels of various cardiolipin (B) and phosphatidylcholine (PC) (C) species in the mitochondrial fraction of BAT from control and Pex16-AKO mice subjected to cold exposure for 2 days. The prefixes “a” and “p” in PC side chains denote alkyl ether and plasmalogen species, respectively; n=9-10. Data are expressed as mean±SEM and were analyzed by Student’s t-test; *p<0.05.

A**B****C****D**

Supplemental Figure 10. Effects of AG on mitochondrial lipids, gene expression, oxygen consumption rate and cold tolerance. (A) Total diacyl and plasmalogen PE levels in the mitochondria from BAT of control and Pex16-AKO mice treated with or without AG; n=5. (B) Gene expression analysis in BAT of cold-treated mice. (C) Oxygen consumption rate (VO₂) measured using indirect calorimetry before and after intraperitoneal norepinephrine (NE) injection in control and Pex16-AKO mice treated with or without AG diet while housed at thermoneutrality for 8 weeks. n=3-4. (D) Cold tolerance was determined by measuring rectal temperature prior to and after 6 hrs of cold exposure in control and Pex16-AKO mice treated with or without AG for 1 week; n=4-6. Data are expressed as mean±SEM and were analyzed by one-way ANOVA, followed by Fisher's LSD test (panels A and D); Student's t-test (panel B); or two-way ANOVA with Bonferroni post test (panel C); *p<0.05; n.s., not significant.



Supplemental Figure 11. Effect of AG on palmitate and pyruvate oxidation in skeletal muscle and liver. (A-D) Palmitate and pyruvate oxidation in skeletal muscle (**A-B**) and liver (**C-D**) of control and Pex16-AKO treated with or without AG diet for 8 weeks; $n=3-4$. (**E**) BAT SVF cells stably expressing lentivirus-encoded myc-Glut4-mCherry were differentiated into adipocytes and then treated with scrambled or Pex16 shRNA. Five days later, the cells were treated with or without insulin after serum starvation and analyzed for Glut4 translocation using confocal microscopy. Exofacial localization of the Myc tag was detected by staining unpermeabilized cells with a rabbit anti-Myc antibody, followed by Alexa Fluor 488 goat anti-rabbit secondary antibody. The fluorescence of mCherry was directly visualized. Quantification of Glut4 translocation is shown to the right of the images. Data are expressed as mean \pm SEM and were analyzed by one-way ANOVA, followed by Fisher's LSD test (panels A-D) or by Student's t-test (panel E); *** $p < 0.001$.

Supplemental Table 1. Sequences of primers of used in quantitative real-time PCR.

Gene Name	Forward (5' to 3')	Reverse (5' to 3')
Acaa1	GTGGCATCAGAAATGGGTCT	GGCTTTCTCACTCTCCAGCA
Acadm	GCCCAGAGAGCTCTAGACGA	CAACCTTCATCGCCATTCT
Acox1	GGATGGTAGTCCGGAGAACA	AGTCTGGATCGTTCAGAATCAAG
Acox2	CCTTCCTAGACCTGCTTCCC	TGTCCGTCATAACAGCCAAG
Acox3	CTTCTGAGAAACGGGGACAA	GCTCGGTAGGCACTAAGAGG
Agps	GTACCAATGAGTGCAAAGCG	CCCCATCCATTCCATTTCAT
aP2	GCGTGGAATTCGATGAAATCA	CCCGCCATCTAGGGTTATGA
CD36	GCGACATGATTAATGGCACA	CCTGCAAATGTCAGAGGAAA
Cpt1	CCTGGGCATGATTGCAAAG	ACGCCACTCACGATGTTCTTC
CS	TGCAGCTGTAGCTCTCTCCC	AAGGACGAGGCAGGATGAG
CtsB	GTTTGGCTTGGTGGCTGC	CAGCAGGCAAGAAAGAAGGA
Cyp4a10	CCCTGATGGACGCTCTTTAC	AGAGTCTGGTGCAAACCTGG
Cyp4a14	GCCATGCTTATCTGCCATTC	ATCTGGCAGCAATTCAAAGC
Drp1	AGATCGTCGTAGTGGGAACG	AGAATGAGAGGTCTCCGGGT
Fis1	ATTTGAATATGCCTGGTGCC	CATAGTCCCGCTGTTCTCT
Gamt	GCAGCCACATAAGGTGTTC	CTCTTCAGACAGCGGGTACG
Gatm	GACCTGGTCTTGTGCTCTCC	GGGATGACTGGTGTGGAGG
Gnpat	CATGGACGTTCCTAGCTCCT	CCCACTTTTGGAGGTCTTTCG
Hsd17b4	AGGCTAGACTCATGGCTTCG	TGAAGTCCCCTCCTAAGTCG
L32	TTCCTGGTCCACAATGTCAA	GGCTTTTCGGTTCTTAGAGGA
LipA	AGTATTCACCGAATCCCTCG	CTAGAATCTGCCAGCAAGCC
Mff	GGAGTTCCAAATGCCAGTGTGATA	TGGATAAGGTCAAGATCTGCTGGT
Mfn1	TGAATAACCGTTGGGATGCT	GCTCCGACGGACTIONTACAAC
Mfn2	GTCCTGGACGTCAAAGGGTA	ATTGATCACGGTGTCTTCC
MT-CO1	TCCTACCACCATCATTTCTCC	CTGATGCTCCTGCATGGG
MT-CO2	CATCAAACCGACCAGGGTT	AATTATTGAAGCAGATCAGTTTTCG
MT-ND6	CCAACATAACTCCAACATCATCA	GTATTGGGGGTGATTATAGAGTTT
Nrf1	TAGTCCTGTCTGGGGAAACC	CTGGTACATGCTCACAGGGA
Opa1	TTTGCAGAAGACGGTGAGAA	TCCTGGTGAAGAGCTTCAATG
Pex13	CCCAAACCTGGGAGTCT	GGGCACTCTGTAAAGTGTGG
Pex16	CCGTTCTATGACCGCTTCTC	GGAGGGCAAGTAGTCCATGA
Pex16 (-4)	GGAGCTCCCGGTCTCGGGAG	CTAAGCCCGCTCCCGGTTG
Pex16 (-601)	GGAGGCCAGCTTAGAACCTG	CGATCTGCACCTCGGGTTTC
Pex16 (-1228)	GGGTTTCTCTGTGTACCTCTGG	GCTCGTTTAACCGGGCAGTG
Pex16 (-1790)	CCTAAGCCAGAGGCAGCTGG	CCTTATCGTTGGATTAGAGTCTG
Pex16 (-2372)	TCTGCTCTTGTCTCTGGAGCC	CCAACAGTGAAGAGTCATCTCTAGG
Pex19	AGCATCATGCAGAACCTCCT	TGCTGCTGCTGGTACTTCTC
Pex7	GAAATTTTCACCGTTCCACG	GTGATGCTCCACTGTTTCCA
Pgc1a	TGTAGCGACCAATCGGAAAT	TGAGGACCGCTAGCAAGTTT
Pmp70	TCTGCCTACTCCATAAGCGG	CACCACAGCTCGCTCTTCT
PPARa	AGTTCGGGAACAAGACGTTG	CAGTGGGGAGAGAGGACAGA
Prdm16	CAGAGGTGTCATCCAGGAG	ACGGATGTACTTGAGCCAGC
RPL30	Cell Signaling Technology, #7015	Cell Signaling Technology, #7015
Ryr2	ATGGCTTTAAGGCACAGCG	CAGAGCCCGAATCATCCAGC

Gene Name	Forward (5' to 3')	Reverse (5' to 3')
Serca2b	ACCTTTGCCGCTCATTTTCCAG	AGGCTGCACACACTCTTTACC
Slc6a8	TGCATATCTCCAAGGTGGCAG	CTACAAACTGGCTGTCCAGA
Tfam	CCAAAAAGACCTCGTTCAGC	GACAGATTTTCCAAGCCTCA
Tomm20	ACTGCATCTACTTCGACCGC	CAGGTAAC TTGGAAAGCCCA
Ucp1	GTACCAAGCTGTGCGATGTC	TCAGCTGTTCAAAGCACACA

Supplemental Methods

Virus Packaging. Plasmids encoding shRNA for mouse Pex16 (18633) and GNPAT (TRCN0000193539) were purchased from Sigma-Aldrich (Saint Louis, MO). Packaging vector psPAX2 (#12260), envelope vector pMD2.G (#12259), and scrambled shRNA plasmid (#1864) were obtained from Addgene. 293T cells in 10 cm dishes were transfected with 2.66 μ g psPAX2, 0.75 μ g pMD2.G, and 3 μ g shRNA plasmid. After 48 hr, media were collected, filtered using 0.45 μ m syringe filters, and used to treat cells. After 36 hr, cells were selected with puromycin and knockdown was assessed after an additional 48 hr or as indicated. To make retroviral particles encoding Cre recombinase, 293T cells in 10 cm dishes were transfected with 3 μ g pBABE-Cre plasmid and 3 μ g ψ A helper plasmid. After 48 hr, media were collected, filtered using 0.45 μ m syringe filters, and used to treat 60% confluent iWAT stromal vascular cells. After 36 hr, the cells were selected with 2 μ g/ml puromycin.

Pex16 Promoter Reporter Assays. COS7 cells were co-transfected with either Pex16-eGFP and empty plasmid or Pex16-eGFP and HA-PRDM16 using Lipofectamine 2000 (Invitrogen). Three days after transfection, the transfected cells were imaged with a Leica DMI4000B inverted fluorescence microscope. For luciferase reporter assays, COS7 cells were co-transfected with Pex16-Luciferase and *Renilla* luciferase plasmids together with either an empty vector or HA-PRDM16. Cells were harvested 3 days later and luciferase reporter assays were performed using the Dual-Glo® Luciferase Assay (Promega, Madison, WI). Firefly luciferase signals were normalized to the *Renilla* luciferase signals.

Gene Expression Analysis by Quantitative RT-PCR. Total RNA from mouse tissues or cells was isolated with PureLink RNA Mini Kit (Life Technologies) and reverse transcribed using High Capacity cDNA Reverse Transcription Kit (Applied Biosystems). For quantitative real-time PCR analysis, PowerUP SYBR Green reagent (Applied Biosystems) was used along with the primers spanning exon-exon boundaries. Relative mRNA expression level was determined using the $2^{(-\Delta\Delta CT)}$ method with ribosomal protein L32 as the internal reference control.

Mitochondrial Redox State Assay. BAT SVF cells stably expressing lentiviral-encoded Mito-roGFP were grown to confluence in a 96-well plate before treatment with differentiation media, as previously described (1). At day 4, the cells were treated with scrambled or Pex16 shRNA lentivirus in the maintenance media. After 24 hr treatment, the viral media were removed and replaced with fresh maintenance media. At day 9 of differentiation, the media were removed and cells were washed once with pre-warmed PBS. The fluorescence of GFP was measured using a 525 nm wavelength emission filter following excitation at 400 nm (oxidative state) or 484 nm (reductive state) using a Tecan Infinite M200 plate reader.

Citrate Synthase Activity. Citrate synthase activity was measured in BAT homogenates using a commercially available kit from Sigma (CS0720). The citrate synthase activity assay was performed in accordance to the manufacturer's instructions. Raw values for citrate synthase activity were normalized to protein content for each sample.

Mitochondrial Membrane Potential Assay. Mitochondrial membrane potential in Pex16 knockdown and control BAT SVF cells was measured using a TMRE Mitochondria Membrane

Potential Assay Kit obtained from Cayman Chemicals (Ann Arbor, MI) according to the manufacturer's instructions. Briefly, BAT SVF cells cultured in 96-well plates were grown to confluence before treatment with differentiation medium, as previously described (1). On 4 days following the initiation of differentiation, the cells were infected with scrambled or Pex16 shRNA lentivirus in the differentiation medium. After 24 hrs, the viral medium was removed and fresh differentiation medium was added. On day 9, the membrane potential-dependent fluorescence of TMRE was measured and normalized to the fluorescence of MitoTracker Green using a Tecan Infinite M200 plate reader. As a positive control for membrane depolarization, the mitochondrial uncoupler carbonyl cyanide 4-(trifluoromethoxy) phenylhydrazone (FCCP) was added.

Mitochondria Isolation. Mitochondria were isolated from BAT as previously reported (2). Briefly, after PBS perfusion, BAT was collected from mice, transferred to 1.5 ml tubes, and minced thoroughly with scissors. The tissue was then transferred to a homogenization tube containing 100 μ l of homogenization buffer (0.25 M sucrose, 20 mM HEPES in distilled H₂O) and homogenized for 10 strokes. The pestle was washed with 800 μ l of homogenization buffer to remove any residual homogenate. The homogenates were transferred to 1.5 ml tubes and vortexed thoroughly before centrifugation at 800 g for 10 min at 4°C. The upper fat cake was removed by forceps and the supernatant (~800 μ l) was transferred to a new tube and centrifuged at 10,000 g for 10 min at 4°C. The supernatant was discarded and the pellet (mitochondrial fraction) was used immediately for lipid extraction or stored at -80°C for future use.

Electrospray Ionization Mass Spectrometry. Lipids were extracted from adipocytes as previously described (3) and analyzed by mass spectrometry. Structural characterization and quantitation of lipids by low-energy CAD tandem mass spectrometry was conducted on a Thermo Scientific (San Jose, CA) TSQ Vantage Triple Stage Quadrupole mass spectrometer equipped with Xcalibur operating system as previously described (4, 5).

Histology. For immunofluorescence analysis of PMP70 in *Pex16-AKO* and control mice, BAT was embedded in Tissue-Tek OCT compound (Sakura Finetek), frozen at -80°C and then 10 µm sections were cut using a Leica cryostat. Sections were placed on glass slides and immunostained using a rabbit anti-PMP70-Atto-488 antibody and images were captured using a Nikon A1Rsi scanning confocal microscope.

Supplemental References

1. Lodhi IJ, Dean JM, He A, Park H, Tan M, Feng C, et al. PexRAP Inhibits PRDM16-Mediated Thermogenic Gene Expression. *Cell Rep.* 2017;20(12):2766-74.
2. Vernochet C, Mourier A, Bezy O, Macotela Y, Boucher J, Rardin MJ, et al. Adipose-specific deletion of TFAM increases mitochondrial oxidation and protects mice against obesity and insulin resistance. *Cell Metab.* 2012;16(6):765-76.
3. Bligh EG, and Dyer WJ. A rapid method of total lipid extraction and purification. *Can J Biochem Physiol.* 1959;37(8):911-7.
4. Brugger B, Erben G, Sandhoff R, Wieland FT, and Lehmann WD. Quantitative analysis of biological membrane lipids at the low picomole level by nano-electrospray ionization tandem mass spectrometry. *Proc Natl Acad Sci U S A.* 1997;94(6):2339-44.
5. Hsu FF, and Turk J. Electrospray ionization with low-energy collisionally activated dissociation tandem mass spectrometry of glycerophospholipids: mechanisms of fragmentation and structural characterization. *J Chromatogr B Analyt Technol Biomed Life Sci.* 2009;877(26):2673-95.